ACS OMEGA

Open Access

http://pubs.acs.org/journal/acsodf

Article

Large-Scale Analysis on Accelerated Aging of Pentaerythritol Tetranitrate (PETN) Powders in Detonators

Kyle D. Spielvogel, Nicholas Lease, Geoffrey W. Brown, Nathan J. Burnside, Maria C. Campbell, and Virginia W. Manner*

Cite This: *ACS Omega* 2024, 9, 32097−32106

Read Online

ACCESS | Metrics & More | Article Recommendations | Supporting Information

ABSTRACT: Pentaerythritol tetranitrate (PETN) has been used extensively in commercial detonators and other explosive applications for many decades. Here, we show the results of a comprehensive 1.5 year aging study of PETN in commercial detonators, addressing batch-to-batch variations, surface area changes, and comparisons of aged loose powders side-by-side with identically aged detonators. Function time analysis of the aged detonators has also been provided and discussed in the context of powder aging. This large-scale, statistically relevant study addresses long-standing questions on PETN aging without the complications from making comparisons between multiple batches of material. We have evaluated the aging time required to reach the maximum measured amount of PETN coarsening and estimated an activation barrier of ∼123 kJ mol^{-1}, which is higher than literature values reported by Gee et al. It is possible that this discrepancy is due to the fact that that this study cannot quantify the relative contributions of surface diffusion versus sublimation processes. At the lower temperatures of 50 and 60 °C, we assume that surface diffusion dominates over sublimation processes, even at longer aging times. At the higher temperature of 75 °C, we assume that both surface diffusion and sublimation contribute at the early time points, which are included in the Arrhenius analysis for coarsening.

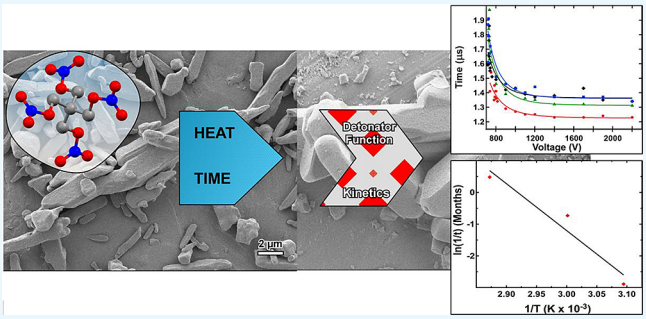

INTRODUCTION

Pentaerythritol tetranitrate (PETN), an explosive organic nitrate, has extensive use in many applications, from blasting caps and detonation fuses to the potential treatment of cardiovascular diseases.[1−4] Current large-scale production of PETN is principally for municipal mining operations and military explosives as the initial pressing in detonators, such as Explosive Bridge Wire (EBW) and Exploding Foil Initiator (EFI) detonators.[1,5−7] The performance of these detonators greatly depends on the average particle size of the loose powders and the density of the pellet that the powders are pressed to.[8−10] However, experimental evidence has shown that PETN particle size, as determined through air permeability measurements, will decrease over time due to powder coarsening resulting from storage or transportation conditions. The addition of naturally occurring homologues, such as tripentaerythritol-octanitrate (triPEON), has been shown to attenuate powder coarsening and is commonly done to preserve detonator function; however, crystal growth has been shown to occur to some degree.[2,11,12] The coarsening of PETN powders, both unstabilized and stabilized by addition of homologues, is well documented and easily investigated by standard analytical methods; nevertheless, there remains a gap of knowledge as to how coarsening of a PETN pellet affects detonator function in a thorough and statistically informed way.

Powder coarsening has been investigated as early as the 1950s through accelerated aging studies that monitored the air permeability of aged powders and function times of resulting pressed detonator pellets.[8,9,13,14] Many studies followed to reproduce this work and generate prediction models to better understand how aging of PETN powders might affect pressing density and detonator performance.[15−18] However, many of these reports used only a small sample size due to the cost and time required to acquire a large amount of detonators. Comparison of results is further complicated as the limited supply of detonator grade PETN powders and varying concentrations of homologues resulted in many studies that contain disparate batches of starting powders at various beginning flow porosities prior to aging. Further questions remain surrounding detonator firing data as pressing the aged material into detonators post aging could arguably result in

Received: May 3, 2024
Revised: June 20, 2024
Accepted: June 26, 2024
Published: July 8, 2024

morphological changes that could affect detonator firing. We recently reported a thermal aging and performance study on four related batches of PETN powder for 1 month of aging.[19] In this study, we extend the aging of two of those batches to 1.5 years, along with kinetic analysis.

In this body of work, we provide a comprehensive aging study that addresses batch-to-batch variations, particle size, and aging comparisons of loose powders side-by-side with identically aged detonators. All PETN powders were sourced from a single feedstock, and the starting particle size of the 1% added triPEON (batch UT) matches as closely as possible to the initial particle size of the uncoated PETN (batch U). Loose powders and detonators were aged alongside one another to provide a good correlation between aging effects and firing characteristics. Powders and disassembled detonators were analyzed by scanning electron microscopy (SEM) imaging and high-performance liquid chromatography (HPLC) with particle size analysis conducted on powders using both light scattering dynamics (Coulter particle size analyzer) and Fisher specific surface area (FSSA). Finally, firing characteristics of the aged detonators were determined by using threshold and voltage sweep firing data. Initial powders were packed into modified commercial RP-2 detonators that permitted the production of 1000 detonators for the collection of statistically significant firing data. The thorough investigation of PETN aging in both powders and detonators that can further inform results from previous historical studies. The kinetic analysis takes this work a step further, with preliminary information on an activation barrier that captures surface diffusion and sublimation processes over the 1.5 year period.

EXPERIMENTAL SECTION

Sample Preparation of Uncoated (U) and TriPEON-Coated (UT) PETN. PETN was obtained from a single cap grade lot and prepared, as described by Lease et al.[19] Uncoated PETN (U) was recrystallized with no stabilizer, and triPEON-coated PETN (UT) was prepared with 1% triPEON. Both U and UT samples were aged as loose powder and pressed inside detonators (modified RP-2 detonators purchased from Teledyne Risi with no output pellets) that were sealed in aluminum cans and aged at three temperatures, 50, 60, and 75 °C. Each set of powder and detonators had three pulls conducted at time points from 1 to 18 months. A detailed schedule of pulls can be found in Table 1.

Table 1. Matrix of Aging Times and Temperatures for U and UT PETN Powders and Detonators

batch	1 month	3 months	9 months	12 months	18 months
U 50 °C	X		X		X
U 60 °C	X	X		X	
U 75 °C	X	X		X	
UT 50 °C	X		X		X
UT 60 °C	X	X		X	
UT 75 °C	X	X		X	

RESULTS

Scanning Electron Microscopy (SEM) Images of Unaged and Aged Powders. Images were collected on all control and aged powder samples in order to compare the crystal morphology variation with aging. The unaged loose powders (Figure 1) exhibit long rod-shaped crystal morphology, with rounded edges for the uncoated powder (U) and sharper edges and more uniform needles in the triPEON-coated powder (UT) (Figure 1). Crystal and particle size information will be discussed in later sections.

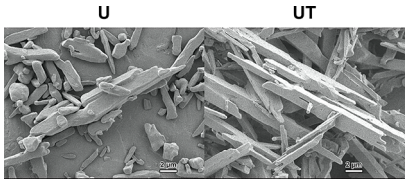

Figure 1. Scanning electron microscopy images of unaged loose powders at 5000× magnification, showing rod-shaped crystals with rounded edges in Batch U (left), compared with those of Batch UT (right) with sharper edges.

Aging of Loose Powders. Upon aging batch U at 50 °C, the samples pulled at 1 and 9 months exhibit an irregular crystal morphology with a few crystals resembling the expected tetragonal crystal habit for PETN (Figure 2). However, at 18 months of aging, the crystals begin to cluster together to form agglomerates as some of the crystals begin to merge and the material coarsens.[20] In addition to the observed coarsening, some of the smaller crystallites begin to display a tetragonal morphology. Agglomeration of the crystals can be observed as early as 1 month of aging in the 60 °C sample, with a significant increase in crystal size observed at 12 months. Notably, at 12 months of aging at 60 °C, the tetragonal crystal morphology becomes more apparent and the smaller particles appear to be integrating into the surface of the larger crystals. The greatest amount of change can be observed in the samples aged at 75 °C. Compared to the irregular morphology observed in the control batch, the crystals largely take on the tetragonal crystal habit with a large increase in crystal size in as little as 1 month of aging. The crystal surfaces for all 75 °C aged samples are smooth with well-defined crystal edges. Further incorporation of smaller crystallites into the larger parent crystals can be observed, likely due to Ostwald ripening.[21−23]

Aging of PETN batch UT at 50 °C showed minute changes, with the overall crystal shape and surfaces being maintained throughout the aging process. After 18 months of aging at 50 °C, the only noticeable difference is a slight rounding of the sharp edges. Aging at 60 and 75 °C does not show largely noticeable differences other than rounding of the sharp crystal edges except for the 75 °C 3 and 12 month images where irregular particle shapes can be observed (Figure 3). However, the images show that the crystal habit of the aged UT samples remains largely unchanged relative to the control sample and is likely due to the reduced amount of sublimation/redeposition compared to that of the uncoated PETN in batch U.

Aging of Detonator Powders. Detonator bodies are described in the previous ref 19. Detonators were disassembled by separating the aluminum body from the header to image the PETN powders within a detonator assembly. Images of unaged batch U and UT detonator powders are shown in Figure 4. Similar to the unaged powders, batch U shows crystals that have rounded edges and mostly irregular crystal habit for the smaller particles with a few larger tetragonal crystals visible within the bulk. Batch UT detonator powder is similar to the loose unaged powder with sharp edges and a more regular crystal habit, even for the smaller particles.

https://doi.org/10.1021/acsomega.4c04251
ACS Omega 2024, 9, 32097−32106

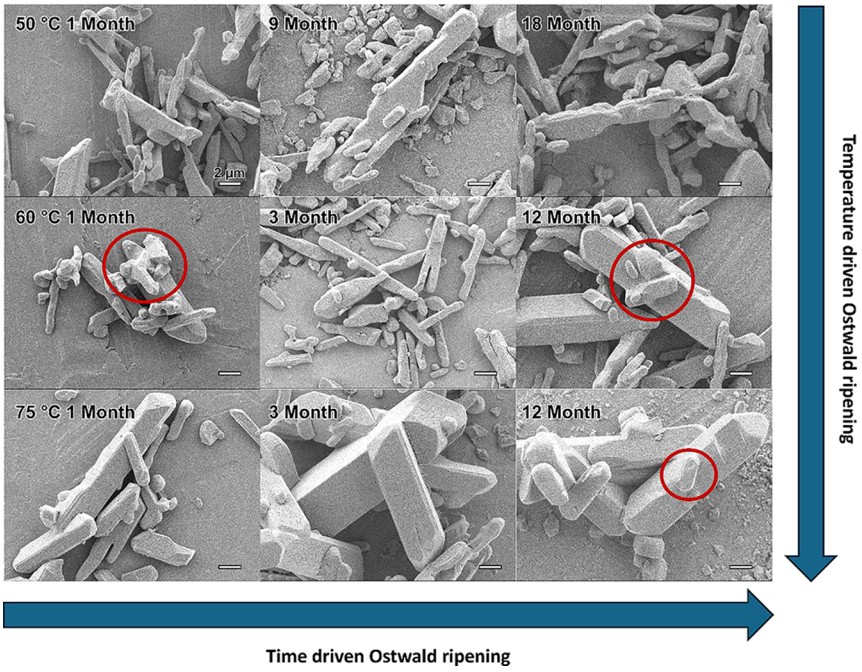

Figure 2. Scanning electron microscopy images of aged batch U loose powders at each temperature, all at 5000× magnification. Arrows denote crystal growth that correlates with Ostwald ripening. Red circles display examples of suspected surface diffusion and the incorporation of smaller crystallites into larger crystals.

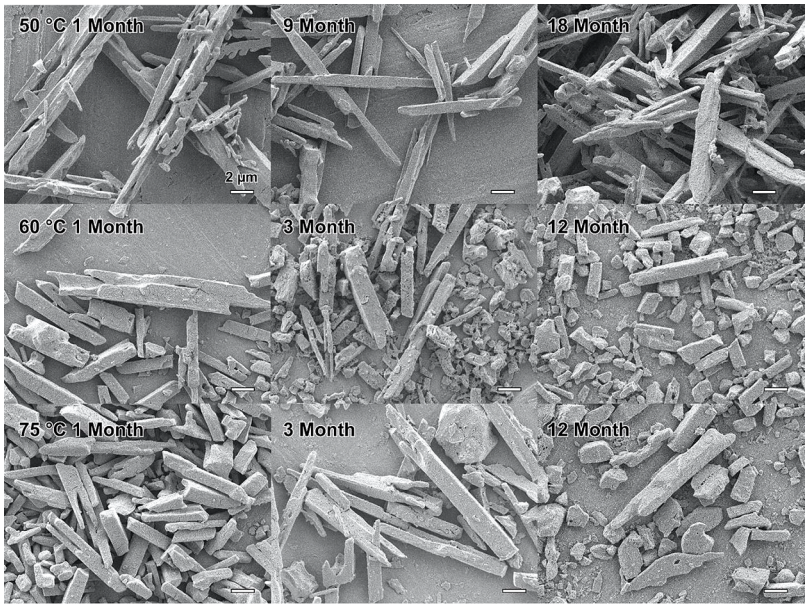

Figure 3. Scanning electron microscopy images of aged batch UT loose powders at 5000× magnification.

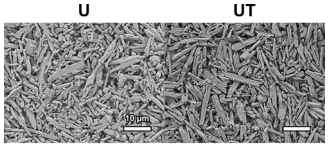

Figure 4. Scanning electron microscopy images of control detonator inputs at 2000× magnification.

SEM images of the powders within the aged detonators show similar sintering and coarsening as with the aged loose powders (Figure 5). Batch U displays an increase in crystal size and irregular crystal habit at the 18 month pull of 50 °C with similar results presenting at the 3 month pull at 60 °C and as early as the 1 month pull at 75 °C. The 3 month pull at 60 °C shows the first evidence of agglomeration and sintering that becomes more apparent at the 12 month time point. The longer aging time results in a large increase in crystal size and incorporation of smaller particles into larger crystals. At 75 °C, the 1 month pull very clearly shows agglomeration and sintering with an observable decrease in the number of smaller particles. The later time points show crystal growth that is likely due to Ostwald ripening and sublimation/redeposition as the crystals appear to be overlapping less, with increasing amounts of clear and identifiable singular tetragonal crystals.

https://doi.org/10.1021/acsomega.4c04251
ACS Omega 2024, 9, 32097−32106

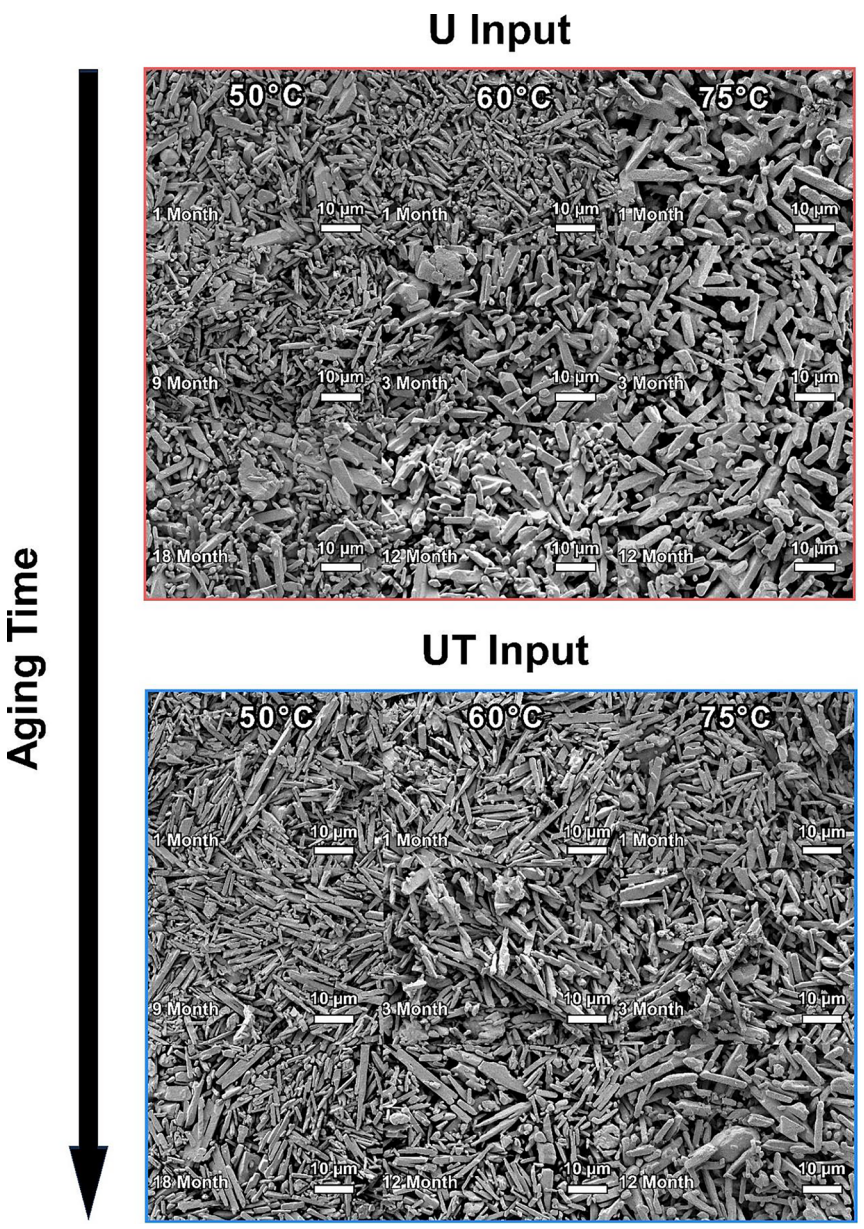

Figure 5. Scanning electron microscopy images of detonator inputs at 2000× magnification.

Particle size remains relatively similar between the aging times and temperatures for UT detonators with significant changes not occurring until the 12 month pull at 60 °C and at each time point at 75 °C. Larger tetragonal crystals become more apparent with the longer aging time, and irregular crystal habit begins to appear at the 75 °C aging temperatures, similar to that of the loose aged powder. Observing these effects within a detonator is important, as detonator function times become slower as particle size increases.

High-Performance Liquid Chromatography (HPLC) Analysis. TriPEON, a homologue of PETN, is present in small amounts in most PETN samples; however, it is not the only homologue commonly observed. Other homologues include diPEHN (dipentaerythritol hexanitrate), tetraPEDN (tetrapentaerythritol dodecanitrate), and PETriN (pentaerythritol trinitrate). Unlike the well-understood ability of triPEON to stabilize PETN powders, ambiguity remains regarding the overall effect diPEHN has on PETN performance. Manufacturing of PETN results in various homologues due to etherification and hydrolysis; however, the addition of diPEHN or triPEON has been shown to reduce PETN vapor pressure, aiding in the stabilization of the crystal surface and inhibiting crystal growth. In this system, HPLC data were collected on all samples of PETN, both loose powders and detonator powders. Because we were more concerned with the changes in PETN homologues; the reported values are relative percents with respect to one another. At every pull, the results showed no observed significant changes in triPEON or diPEHN with aging at any temperature for both U and UT batches. The relatively flat percentages of triPEON and diPEHN with aging are shown in Figure 6. Previous work has studied the effects of homologue levels on detonator performance[2,11]; however, the data shown here demonstrate no major changes in homologue levels with aging time.

Particle Size Distribution Analysis of U and UT Powders. All sample pulls were evaluated for particle size characteristics through a light scattering technique (Coulter particle size analyzer). Table 2 shows the particle size statistical

https://doi.org/10.1021/acsomega.4c04251
ACS Omega 2024, 9, 32097−32106

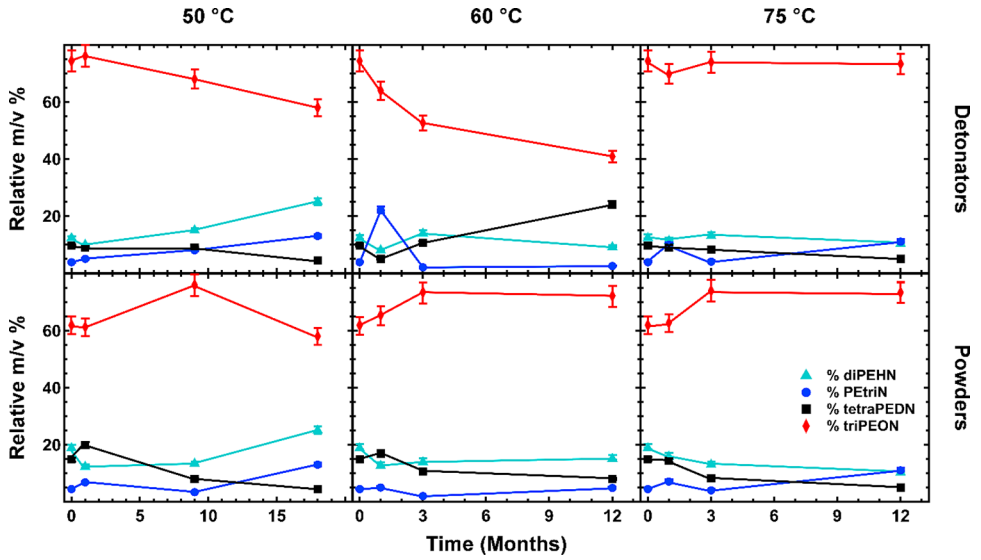

Figure 6. High-performance liquid chromatography values of various pentaerythritol tetranitrate (PETN) homologues after each aging pull, relative to PETN as relative m/v %, showing no significant changes for each. Error bars are shown as a 5% standard error.

Table 2. Unaged Particle Size Distribution Analysis of Uncoated PETN and 1% Added TriPEON-Coated PETN[a]

batch	$D_{[4,3]}$	span	D_{10}	D_{25}	D_{50}	D_{75}	D_{90}
U	431.4	10.8	3.22	6.89	16.21	40.93	178.69
UT	95.1	2.3	5.77	10.95	19.63	34.17	51.52

[a]Reported values are in μm.

distribution of the unaged samples for U and UT. Particle size analysis of the unaged powders resulted in slight differences between the U and UT batches. Unaged samples of batch U showed irregular grain size throughout the bulk powder, reflected by the calculated span value (eq 1) of 10.8 (where span → 0 means less variation in particle size) and the multiple peaks present in the black trace of Figure 7.[24]

$$\text{Span} = \frac{D_{v0.9} - D_{v0.1}}{D_{v0.5}} \quad (1)$$

The samples containing 1% triPEON exhibit a more uniform distribution, with fewer peaks in the red trace and a calculated span value of 2.3. The batches display a varied $D_{[4,3]}$ (mass moment mean) with batch U at 431.4 μm and batch UT at 95.1 μm that exemplifies the nominally smaller average particle size of the UT batch relative to the U batch.

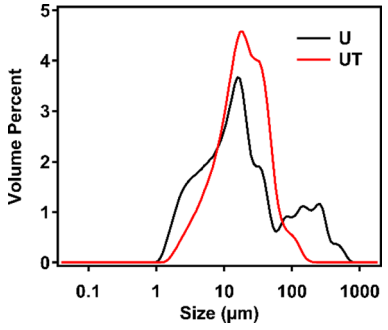

Figure 7. Coulter particle size analysis plot of unaged uncoated pentaerythritol tetranitrate (PETN) (U) and PETN coated with 1% added triPEON (UT) control powders.

As shown in Figure 8, large particle growth is observed in the U batch as time and temperature increase, with an increased population of particles sized between 200 and 1000 μm in as little as 1 month. All particle size statistics are presented in Table S8 of the Supporting Information. Figure 9 shows the changes in $D_{[4,3]}$ with aging for each batch of U and UT powder. At the higher temperature aging of 75 °C, the $D_{[4,3]}$ values have a linear increase in particle size, suggesting that the thermophysical processes taking place are occurring at a constant rate. However, the lower temperatures (50 and 60 °C) show random particle growth occurs with aging.

Aged samples of batch UT show the stabilizing ability of added triPEON, with little change at 50 and 60 °C, and a largely attenuated change within the 75 °C sample in comparison to batch U (Figures 8 and 9). The resulting data display an approximate Gaussian distribution, as seen by the relatively similar span values averaged around 2.4 (±0.3), and allow for the analysis of the mode value (particle size with the largest population) in addition to the $D_{[4,3]}$. Samples aged at 75 °C show some initial growth during aging from 1 to 12 months, with the mode value increasing to about 25 μm (12 months) and an increase in the $D_{[4,3]}$ value from 95 μm (1 month) to 129 μm (12 months). At lower temperatures, these changes with aging are significantly smaller. At all temperatures, the increased population of larger particles appears to be from a slight loss of smaller particles between 1 and 10 μm, as seen in the traces in Figure 8. However, the span value does not change greatly, suggesting that the aging process is uniform within the sample. Overall, it is clear that the particle size changes with thermal aging in the UT batch are significantly smaller than observed in the U batch, consistent with the well-known stabilization of PETN seen with triPEON in multiple previous studies by Gee and Foltz et al. However, quantifying this aging using Coulter is difficult due to sintering of smaller particles into agglomerates during the aging process.

Fisher Specific Surface Area (FSSA) Analysis of Loose Powders. A Fisher subsieve sizer was used to collect measurements to determine the air permeability of a powder bed, giving an average particle size which is reported as the FSSA (in units of cm^2 g^{-1}). FSSA measurements were

https://doi.org/10.1021/acsomega.4c04251
ACS Omega 2024, 9, 32097−32106

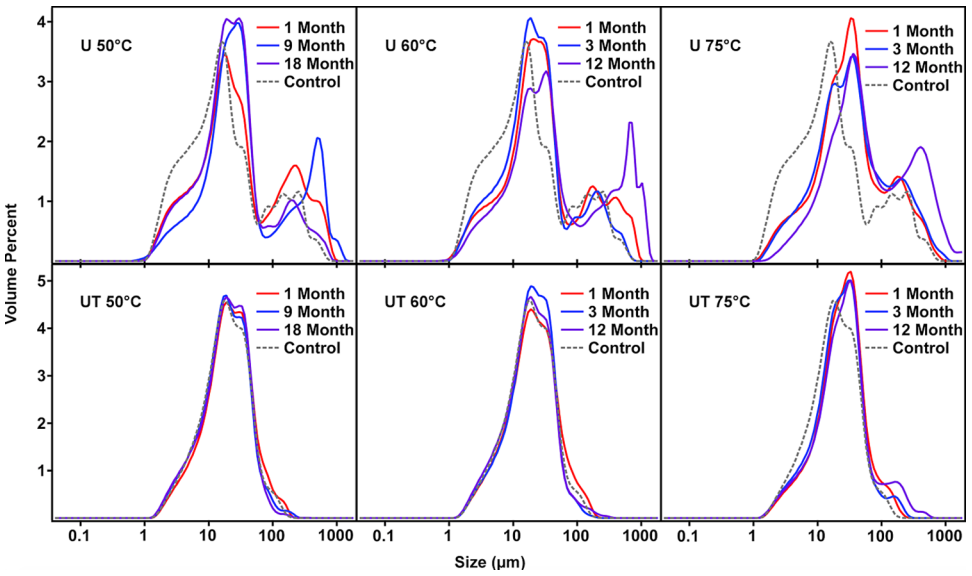

Figure 8. Coulter particle size analysis plots of U and UT after aging at 50, 60, and 75 °C.

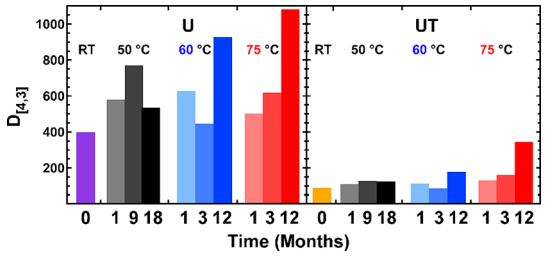

Figure 9. Histogram depicting the mass moment mean ($D_{[4,3]}$) particle size with aging.

conducted for each time point and compared against the control values to determine the amount of coarsening with temperature. Analysis of PETN aging by FSSA must be approached with caution as compaction during the sample preparation process could crush larger crystallites and break up weakly bound sintered particles that would artificially raise the overall powder surface area.[25] However, FSSA still proves to be a useful qualitative technique to connect similarly aged PETN powders and detonators to the detonator function time. Values in Table 3 contain standard deviation of the mean error values after duplicate runs, and the plotted data in Figure 10 contain a 2.06% relative standard deviation error that was applied from the sample with the highest error.

Table 3. Fisher Specific Surface Area Values ($cm^2\ g^{-1}$), with the Average and Standard Deviation of the Mean from Two Separate Runs

temperature	time	U	UT
N/A	control	12,980 ± 90	14,127 ± 1
50	1 month	11,640 ± 70	13,557 ± 1
	9 months	11,160 ± 70	14,898 ± 1
	18 months	9800 ± 200	13,424 ± 1
60	1 months	10,271 ± 3	13,034 ± 1
	3 months	9400 ± 100	12,970 ± 90
	12 months	9224 ± 2	13,559 ± 2
75	1 month	7840 ± 60	12,000 ± 200
	3 months	7170 ± 70	11,489 ± 1
	12 months	5870 ± 70	9860 ± 50

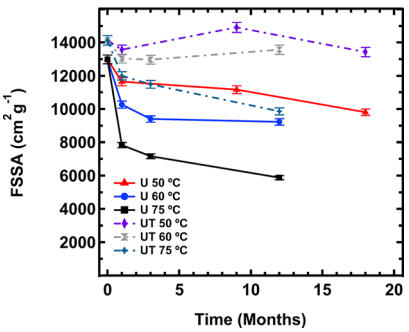

Figure 10. Fisher specific surface area for U and UT batches of PETN samples at each temperature and time point.

As seen in the particle size distribution data, unaged batch U has a lower initial specific surface area at 12,980 $cm^2\ g^{-1}$ compared to that of batch UT at 14,127 $cm^2\ g^{-1}$. Both batches coarsen at each temperature and exhibit a sharp decrease in surface area at the first pull time, something that has been observed by Dinegar, Foltz, and others in similar studies.[14−16] Batch U shows a large decrease in surface area at 1 month, with decreases of 1340, 2709, and 5140 $cm^2\ g^{-1}$ at 50, 60, and 75 °C, respectively. Though there are only three time points available for analysis, the coarsening observed at the lower temperatures of 50 and 60 °C appears to slow at the 12−18 month time points, while the 75 °C sample appears to continue to exhibit coarsening at the last time point of 12 months. This suggests the possibility that the dominant mechanism of aging at lower temperatures is the result of slow surface diffusion and migration. At higher temperatures, it is likely that there is enough energy to favor sublimation/redeposition in addition to surface diffusion and migration. Aging studies at temperatures between 60 and 75 °C, as well as longer times, are needed to deconvolute these two contributing mechanisms.

While the 50 °C data for batch UT show varied results, the 9 months pull time displays a slightly increased surface area that

https://doi.org/10.1021/acsomega.4c04251
ACS Omega 2024, 9, 32097−32106

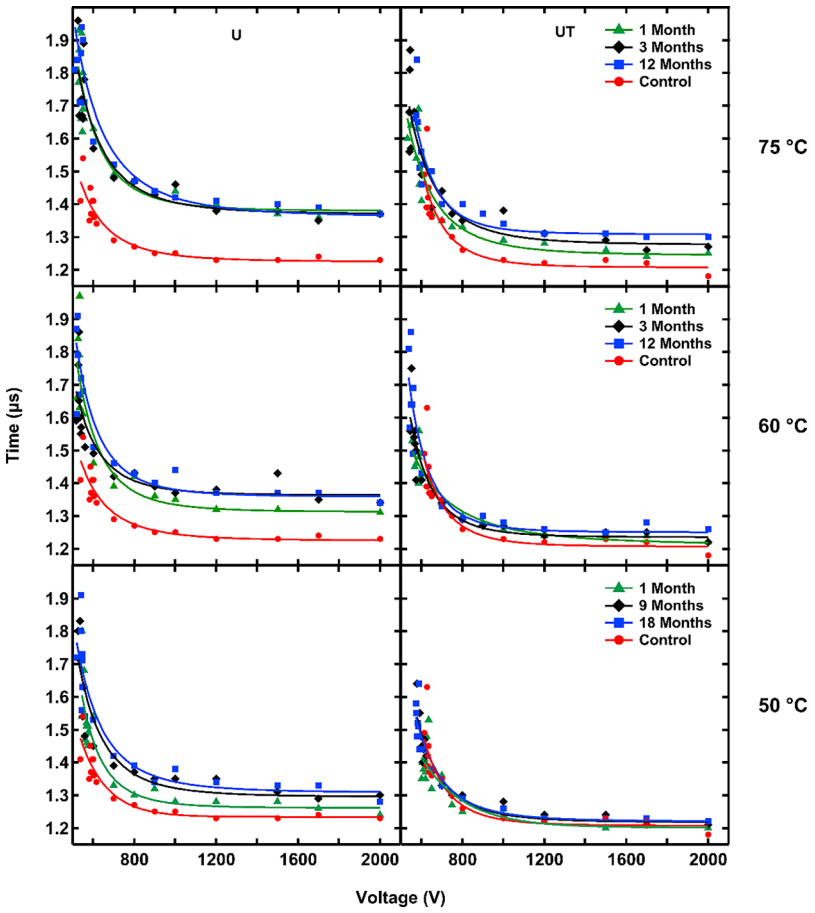

Figure 11. Detonator function time vs input voltage of U and UT after aging at 50, 60, and 75 °C.

is greater than that of the control powder, which is evidence of the typical measurement error using this method. At 1 month, batch UT exhibits a decrease of 570, 1039, and 2127 $cm^2\ g^{-1}$ for 50, 60, and 75 °C, respectively. However, the continued aging becomes insignificant for 50 and 60 °C as the later sample values are within error. At 75 °C, batch UT continues to age in an approximately linear fashion, suggesting that aging at longer time points is needed to determine when the coarsening begins to slow. However, the overall attenuated coarsening of batch UT compared with batch U confirms the triPEON stabilization of PETN powders.

Detonator Performance Testing. Studies on EBW detonators have shown a strong correlation between FSSA and detonator function time (time from bridge burst to the detonation wave leaving the detonator).[9,10,13,17,26] At elevated temperatures, PETN has been shown to undergo Ostwald ripening (as shown above and in previous reports) that results in a larger particle size within a detonator configuration and in loose powders. Powder morphology is known to directly affect the detonation performance. For example, particle size may affect the voltages required for the minimum input energy to initiate a detonation from the bridgewire burst (threshold voltage), and larger particles typically result in lengthening the time between the bridgewire burst and the detonator breakout recorded by the piezo foil signal (function time).[9,10,26,27]

Input voltage and function timing were thoroughly investigated by conducting 25 shots for every temperature and PETN batch. The EBW detonators were fabricated and tested, as previously described.[19] Shots were conducted by investigating function times during threshold (500−800 V), as well as voltage sweeps and hardfire (1200−2000 V) to assess how the detonation performance is affected by prolonged aging. The detonators were aged with the powders (1, 3, 9, 12, and 18 months) with the pull times dictated by the aging temperature (50, 60, and 75 °C).

Function times were collected for both the U and UT batches. At hardfire conditions, unaged U and UT batches exhibited similar function times of 1.23 ± 0.01 and 1.22 ± 0.02 μs, respectively. However, differences could be observed in threshold voltages: U detonators exhibited lower threshold voltages for initiation, at 550 ± 20 V, compared to UT at 620 ± 10 V, albeit with a similar breakout time (1.39 ± 0.09 μs).

At hardfire input voltages, batch U function times increase with aging, reaching a maximum function time of 1.38 μs (Figure 11). Aging at 50 °C for 18 months does not reach this maximum value, with a function time of 1.33 μs. However, through aging at 60 °C, the maximum function time is reached within 3 months. At 75 °C, batch U reaches the maximum function time within 1 month of aging, and further, aging does not result in an increase in function time, even with the continued coarsening observed in FSSA measurements (Figure 10, black trace). The increase in function time of 0.15 μs does not result in unusable detonators but is outside the specifications of typical commercial detonators (Teledyne Risi detonators generally have a standard deviation of 0.035 μs or less). The threshold voltages (Table 4) (SI; Tables S1−S7) for batch U at 75 °C are unaffected during the aging process.

https://doi.org/10.1021/acsomega.4c04251
ACS Omega 2024, 9, 32097−32106

Table 4. Threshold Values of Batch U and Batch UT (in V)

temperature	pull time	U	UT
control		550 ± 20	620 ± 10
50 °C	1 month	549 ± 9	610 ± 20
	9 months	540 ± 20	590 ± 10
	18 months	530 ± 20	578 ± 6
60 °C	1 month	522 ± 7	570 ± 10
	3 months	522 ± 6	540 ± 10
	12 months	520 ± 10	550 ± 20
75 °C	1 month	530 ± 10	560 ± 30
	3 months	530 ± 10	539.6 ± 0.2
	12 months	520 ± 20	570 ± 20

Batch UT function times at hardfire voltages also increase with aging, reaching a maximum function time of 1.30 μs (at 12 months, 75 °C). However, at each temperature, batch UT detonators age at much slower rates compared to that of batch U detonators. Aging at 50 °C results in hardfire function times within error of the unaged detonators at 1.22 μs, and aging at 60 °C for 12 months results in detonator function times of 1.26 μs. Averaged threshold voltages for aged UT detonators are slightly lower, at 550 V compared to that of the control batch at 620 V (Table 4). However, aging does not result in a discernable trend in threshold voltages.

DISCUSSION

Comparison of FSSA results versus the function time at multiple voltages generates the plot shown in Figure 12A (originally developed by Dinegar), where increased coarsening (lower FSSA values) correlates with a longer function time. Batch U powder begins with a FSSA value of ~13,000 $cm^2\ g^{-1}$ and a function time of 1.23 μs, and as the PETN coarsens, the function time increases to a maximum of 1.38 μs. Interestingly, this maximum function time is reached within the 3 months period of aging at 60 °C with a FSSA of 9400 $cm^2\ g^{-1}$. Despite continued coarsening observed through FSSA values at 75 °C over the 12 month period, with a minimum value of ~6100 $cm^2\ g^{-1}$, the function time under hardfire conditions does not continue to increase after 1 month of aging. It is important to note that these detonators were prepared specifically for this study, with only PETN input pellets and no high-density output pellets. To connect these results with traditional commercial detonators, output pellets would need to be incorporated in future studies.

We have fit an Arrhenius model to the FSSA aging data using the three aging temperatures of batch U. Batch UT exhibits aged FSSA values that were insignificant at lower temperatures, resulting in a model that could not be reliably fit and suggests that future studies should incorporate a greater number of samples at longer times for analysis. Batch U proved to be more amenable to a first order Arrhenius model. Ideally, the fit would incorporate the FSSA value where the maximum detonator hardfire delay time occurred in the 60 °C sample at 9400 $cm^2\ g^{-1}$; however, this value could not be captured in the 50 °C aging data. Alternatively, we have chosen to evaluate the aging time required to reach 9800 $cm^2\ g^{-1}$, the final FSSA value obtained for the lowest temperature aging (Figure 12B, dashed purple line), thereby allowing for a comparison between the different temperatures. Plotting the time points for this value results in the Arrhenius plot in Figure 12C and an activation barrier of ~123 kJ mol^{-1}. This value is higher than literature values reported by Gee et al. at ~50 kJ mol^{-1}.[17] It is important to note that this study cannot quantify the relative contributions of what we assume to be faster surface diffusion versus slower sublimation processes that can occur over longer periods of time. This is a possible explanation for why the activation barrier found for this study is larger than the value found by Gee et al. Furthermore, a recent study on sublimation in PETN nanofilms reported activation barriers of roughly 126 kJ mol^{-1}, in reasonable agreement with our estimate.[28] At the lower temperatures of 50 and 60 °C, we assume that surface diffusion dominates over sublimation processes, even at the longer aging times. At the higher temperature of 75 °C, we assume that both surface diffusion and sublimation contribute at the early time points, which is inherently included in the Arrhenius analysis for coarsening and results in a larger E_a value.

CONCLUSIONS

In summary, we have conducted a large-scale, multianalytical, and statistically significant accelerated aging study of uncoated (U) and 1% triPEON stabilized PETN (UT). While analysis of aged PETN powders by HPLC and Coulter particle size analysis did not contribute to our understanding of aging and powder coarsening, the data serve as a potential baseline for further investigation in future studies. Similar to previous studies conducted by Dinegar, the FSSA proved to be the most useful method for connecting aging effects of powders to detonator firing results for the U batch. There appears to be multiple mechanistic pathways for powder coarsening, which we assume to be surface migration and sublimation. However, in order to fill an important gap in this field, this study prioritized statistically significant results in detonator firing data (using approximately 1000 detonators) rather than longer aging times and more aging temperatures. It is important to note that accelerated aging at higher temperatures (such as 75

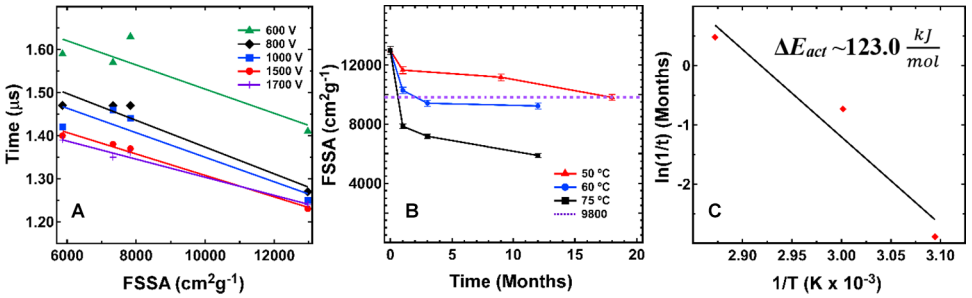

Figure 12. Dinegar plot (A), fisher specific surface area plot with selected size for analysis in purple dashed line (B), and first order Arrhenius plot at 9400 $cm^2\ g^{-1}$ for batch U data, with ΔE_{act} ~ 123.0 kJ/mol (C).

https://doi.org/10.1021/acsomega.4c04251
ACS Omega 2024, 9, 32097−32106

°C) may introduce different mechanisms of PETN coarsening that might not be observed under lower temperature conditions. Future studies including more coarsening data at both shorter and longer times will be important for determining the interplay of surface migration and sublimation to generate better models for the prediction of aging characteristics.

■ ASSOCIATED CONTENT

Supporting Information

The Supporting Information is available free of charge at https://pubs.acs.org/doi/10.1021/acsomega.4c04251.

Function time values, SEM images, and particle size information (PDF)

■ AUTHOR INFORMATION

Corresponding Author

Virginia W. Manner − *High Explosives Science & Technology, Los Alamos National Laboratory, Los Alamos, New Mexico 87545, United States;* orcid.org/0000-0002-1916-4887; Email: vwmanner@lanl.gov

Authors

Kyle D. Spielvogel − *High Explosives Science & Technology, Los Alamos National Laboratory, Los Alamos, New Mexico 87545, United States*

Nicholas Lease − *High Explosives Science & Technology, Los Alamos National Laboratory, Los Alamos, New Mexico 87545, United States;* orcid.org/0000-0001-5932-8885

Geoffrey W. Brown − *High Explosives Science & Technology, Los Alamos National Laboratory, Los Alamos, New Mexico 87545, United States*

Nathan J. Burnside − *Detonation Science and Technology, Los Alamos National Laboratory, Los Alamos, New Mexico 87545, United States*

Maria C. Campbell − *High Explosives Science & Technology, Los Alamos National Laboratory, Los Alamos, New Mexico 87545, United States*

Complete contact information is available at: https://pubs.acs.org/10.1021/acsomega.4c04251

Notes

The authors declare no competing financial interest.

■ ACKNOWLEDGMENTS

This work was supported by the US Department of Energy through the Los Alamos National Laboratory. Los Alamos National Laboratory is operated by Triad National Security, LLC, for the National Nuclear Security Administration of U.S. Department of Energy (Contract No. 89233218CNA000001). The authors would like to thank the Detonation Science and Technology group and the LANL Aging and Lifetimes Program for funding and Spencer Anthony, Taylor Dehner, Kristina Gonzales, Patricia Huestis, and Hongzhao Tian for contributed efforts for the collection of analytical data and editorial conversations. Approved for public release: LA-UR-24-21560.

■ REFERENCES

(1) Rae, P. J.; Dickson, P. M. A review of the mechanism by which exploding bridge-wire detonators function. *Proceedings of the Royal Society A: Mathematical, Physical and Engineering Sciences* **2019**, *475* (2227), No. 20190120.

(2) Bhattacharia, S. K.; Maiti, A.; Gee, R. H.; Weeks, B. L. Sublimation properties of pentaerythritol tetranitrate single crystals doped with its homologs. *Propellants, Explosives, Pyrotechnics* **2012**, *37* (5), 563−568.

(3) Fraccarollo, D.; Galuppo, P.; Neuser, J.; Bauersachs, J.; Widder, J. D. Pentaerythritol tetranitrate targeting myocardial reactive oxygen species production improves left ventricular remodeling and function in rats with ischemic heart failure. *Hypertension* **2015**, *66* (5), 978−987.

(4) Giles, T. D.; Iteld, B. J.; Quiroz, A. C.; Mautner, R. K. The prolonged effect of pentaerythritol tetranitrate on exercise capacity in stable effort angina pectoris. *Chest* **1981**, *80* (2), 142−145.

(5) Davies, H. R.; Chapman, D. J.; Vine, T. A.; Proud, W. G. Characterisation of an exploding foil initiator (efi) system. *AIP Conf. Proc.* **2009**, *1195* (1), 283−286.

(6) Lee, E. A.; Drake, R. C.; Richardson, J. A view on the functioning mechanism of ebw detonators-part 3: Explosive initiation characterisation. *Journal of Physics: Conference Series* **2014**, *500* (18), No. 182023.

(7) Varosh, R. Electric detonators: Ebw and efi. *Propell., Explos., Pyrotech.* **1996**, *21* (3), 150−154.

(8) Aslam, T. D.; Bolme, C. A.; Ramos, K. J.; Cawkwell, M. J.; Ticknor, C.; Price, M. A.; Leiding, J. A.; Sanchez, N. J.; Andrews, S. A. Shock to detonation transition of pentaerythritol tetranitrate (petn) initially pressed to 1.65 g/cm3. *J. Appl. Phys.* **2021**, *130* (2), No. 025901.

(9) Dinegar, R. H. Effect of precipitation on the specific surface and explosive characteristics of petn. In *Conference: International Pyrotechnics Society symposium*; Karlsruhe, F. R., Ed.; Germany, United States, 1985.

(10) Dinegar, R. H.; Rochester, R. H.; Millican, M. S. *The effect of specific surface on the explosion times of shock initiated petn*; LADC-5776; CONF-117-1, 1963. https://www.osti.gov/biblio/12673347. https://www.osti.gov/servlets/purl/12673347.

(11) Bhattacharia, S. K.; Maiti, A.; Gee, R. H.; Nunley, J.; Weeks, B. L. Effect of homolog doping on surface morphology and mass-loss rates from petn crystals: Studies using atomic force microscope and thermogravimetric analysis. *Propellants, Explosives, Pyrotechnics* **2014**, *39* (1), 24−29.

(12) Om Reddy, G.; Srinivasa Rao, A. Stability studies on pentaerythritol tetranitrate. *Propellants, Explosives, Pyrotechnics* **1992**, *17* (6), 307−312.

(13) Blackburn, J. H.; Reithel, R. J. *Exploding wire detonators: Sweeping-image photographs of the exploding bridge wire initiation of petn.; LADC-6288; CONF-533−2*; United States, 1964. https://www.osti.gov/biblio/4043737. https://www.osti.gov/servlets/purl/4043737.

(14) Rogers, R. N.; Dinegar, R. H. Thermal analysis of some crystal habits of pentaerythritol tetranitrate. *Thermochim. Acta* **1972**, *3* (5), 367−378.

(15) Foltz, M. F. Aging of pentaerythritol tetranitrate (petn). In *Aging of Pentaerythritol Tetranitrate (PETN)*; 2009.

(16) Maiti, A.; Gee, R. H. Petn coarsening - predictions from accelerated aging data. *Propellants, Explosives, Pyrotechnics* **2011**, *36* (2), 125−130.

(17) Maiti, A.; Olson, T. Y.; Han, T. Y.; Gee, R. H. Long-term coarsening and function-time evolution of an initiator powder. *Propellants, Explosives, Pyrotechnics* **2017**, *42* (12), 1352−1357.

(18) Makashir, P. S.; Kurian, E. M. Spectroscopic and thermal studies on pentaerythritol tetranitrate (petn). *Propellants, Explosives, Pyrotechnics* **1999**, *24* (4), 260−265.

(19) Lease, N.; Burnside, N. J.; Brown, G. W.; Lichthardt, J. P.; Campbell, M. C.; Buckley, R. T.; Kramer, J. F.; Parrack, K. M.; Anthony, S. P.; Tian, H.; et al. The role of pentaerythritol tetranitrate (petn) aging in determining detonator firing characteristics. *Propellants, Explosives, Pyrotechnics* **2021**, *46* (1), 26−38.

(20) Nichols, G.; Byard, S.; Bloxham, M. J.; Botterill, J.; Dawson, N. J.; Dennis, A.; Diart, V.; North, N. C.; Sherwood, J. D. A review of the terms agglomerate and aggregate with a recommendation for nomenclature used in powder and particle characterization. *J. Pharm. Sci.* **2002**, *91* (10), 2103−2109.
(21) Baldan, A. Review progress in ostwald ripening theories and their applications to nickel-base superalloys part i: Ostwald ripening theories. *J. Mater. Sci.* **2002**, *37* (11), 2171−2202.
(22) Hikal, W. M.; Bhattacharia, S. K.; Peterson, G. R.; Weeks, B. L. Controlling the coarsening stability of pentaerythritol tetranitrate (petn) single crystals by the use of water. *Thermochim. Acta* **2012**, *536*, 63−67.
(23) Marsh, S. P.; Glicksman, M. E. Kinetics of phase coarsening in dense systems. *Acta Mater.* **1996**, *44* (9), 3761−3771.
(24) Lee Black, D.; McQuay, M. Q.; Bonin, M. P. Laser-based techniques for particle-size measurement: A review of sizing methods and their industrial applications. *Prog. Energy Combust. Sci.* **1996**, *22* (3), 267−306.
(25) Maiti, A.; Han, Y.; Zaka, F.; Gee, R. H. In-situ monitoring of flow-permeable surface area of high explosive powder using small sample masses. *Propellants, Explosives, Pyrotechnics* **2015**, *40* (3), 419−425.
(26) Dinegar, R. H. The effects of heat on pentaerythritol tetranitrate (petn). In *Proceedings of the 12th International Pyrotechnics Seminar*; 1987.
(27) Burritt, R.; Bowden, M. The effect of surface area and density on the volumetric shock initiation of petn. *AIP Conf. Proc.* **2020**, *2272*, No. 050007.
(28) Kosareva, E.; Gainutdinov, R.; Nikolskaia, A.; Pivkina, A. N.; Muravyev, N. V. Can the sublimation enthalpy be obtained using atomic force microscopy with heating? A petn nanofilm case. *Langmuir* **2023**, *39* (26), 9035−9043.

https://doi.org/10.1021/acsomega.4c04251
ACS Omega 2024, 9, 32097−32106